Eur. Phys. J. A (2014) **50**: 167
DOI 10.1140/epja/i2014-14167-9

THE EUROPEAN PHYSICAL JOURNAL A

Regular Article – Theoretical Physics

Density and temperature in heavy-ion collisions: A test of classical and quantum approaches

H. Zheng[1,2,a], G. Bonasera[1,2], J. Mabiala[1], P. Marini[3], and A. Bonasera[1,4]

[1] Cyclotron Institute, Texas A&M University, College Station, TX 77843, USA
[2] Physics Department, Texas A&M University, College Station, TX 77843, USA
[3] CENBG, Université de Bordeaux, CNRS/IN2P3, Chemin du Solarium, BP 120, 33175 Gradignan, France
[4] Laboratori Nazionali del Sud, INFN, via Santa Sofia, 62, 95123 Catania, Italy

Received: 26 August 2014 / Revised: 19 October 2014
Published online: 4 November 2014 –
Communicated by F. Gulminelli

Abstract. Different methods to extract the temperature and density in heavy-ion collisions (HIC) are compared using a statistical model tailored to reproduce many experimental features at low excitation energy. The model assumes a sequential decay of an excited nucleus and a Fermi-gas entropy. We first generate statistical events as a function of excitation energy but stopping the decay chain at the first step. In such a condition the "exact" model temperature is determined from the Fermi-gas relation to the excitation energy. From these events, using quantum fluctuation (QF) and classical fluctuation (CF) methods for protons and neutrons, we derive temperature and density (quantum case only) of the system under consideration. Additionally, the same quantities are also extracted using the double ratio (DR) method for different particle combinations. A very good agreement between the "exact" model temperatures and quantum fluctuation temperatures is obtained. The role of the density is discussed. Classical methods give a reasonable estimate of the temperature when the density is very low, as expected. The effects of secondary decays of the excited fragments are discussed as well.

1 Introduction

The investigation of the nuclear equation of state (NEOS) is one of the most challenging open problems today, in particular the access to the symmetry energy part which carries relevant information, especially for the nuclear (astro) physics domain [1–5]. A feasible way to experimentally constrain the NEOS is through the heavy-ion collisions (HIC) at intermediate energies involving nuclei with a large range of N/A ratios. The systems created in such conditions are dynamical and strongly influenced by the Coulomb interaction, angular momentum and other effects, thus the determination of "quasi-equilibrium" conditions is rather challenging. The NEOS can be determined if we are able to extract the temperature, density and pressure, or free energy from the HIC data. Several methods can be found in the literature to determine such quantities from available experimental data. Classical approaches include slope temperature from the kinetic energy distribution of emitted ions [6–8], excited level energy distributions [9] and double isotopic ratios [6–15]. In particular, the last method provides information on the density ρ of the system at the time when fragments are emitted from a source at a given excitation energy per particle $\frac{E^*}{A}$. A coalescence approach [13–19] can also be used to estimate the density of the system. Even though such a method is derived from classical physics, the obtained densities are higher than those from the double ratio (DR) method [13–15, 20]. This might be due to the introduction of a new parameter (the coalescence radius P_0) which is determined from experimental data. Such a parameter might in fact mimic important quantum effects [20] which result in a generally higher density, for a given temperature T, as compared to the one obtained from the DR method. More recently, a different method to extract T and ρ from the data has been proposed in [21–26] based on fluctuations. The method was first used for quadrupole fluctuations within a classical approach, in order to obtain the temperature of the system. Later on this method was applied to quantum systems for which the temperature is naturally connected to the density. In such a scenario, particle multiplicity fluctuations are used in order to pin down T and ρ from experimental data and modeling [22–30]. An important first distinction between fermions and bosons is necessary in order to evidence important quantum effects such as the normalized multiplicity fluctuations $\frac{\langle(\Delta N)^2\rangle}{\bar{N}}$.

[a] e-mail: zhengh@physics.tamu.edu

For fermions they are always smaller than one, which is fermion quenching (FQ), while for bosons they might diverge near the critical point for the Bose-Einstein Condensation (BEC). These phenomena have been observed in trapped Fermi and Boson gases [31–34], and also in heavy-ion collisions [30,35]. A correction due to Coulomb effects for bosons and fermions was also introduced in refs. [2,25,26].

2 Methods

In order to distinguish among different approaches and test their region of validity, we have applied the DR method, the classical fluctuation (CF) and quantum fluctuation (QF) methods to analyze "events" obtained from a commonly used statistical model dubbed as GEMINI [36–43]. Similar studies using the slope temperature have been reported in refs. [44,45]. The model assumes a sequential statistical decay of a hot source of mass (A) and charge (Z), with $\frac{E^*}{A}$ and a given total angular momentum J, which we assume equal to zero for simplicity in this work. We fix $A = 80$ and $Z = 40$ also in order to compare to many calculations based on the Constrained Molecular Dynamical model (CoMD) which we have performed before [22–28]. The statistical model assumes that a hot source decays into a small fragment (A', Z') and a daughter nucleus $(A - A', Z - Z')$. In general both fragments can still be excited and decay again into other fragments and so on until all excitation energy is transformed into kinetic energy of fragments and the Q-value determined from the initial source and the final fragments. At each decay step, the probability of the process is determined from the entropy which is assumed to be that of a Fermi gas [46,47]:

$$S = 2aT, \tag{1}$$

corresponding to an excitation energy

$$E^* = aT^2. \tag{2}$$

Both equations can be derived from a simple low temperature approximation of a Fermi gas. The level density parameter a in such approximation is given by

$$a = \frac{A}{k}\,, \tag{3}$$

where $k = 15(\frac{\rho}{\rho_0})^{2/3}$ MeV. In order to take into account experimental observations, *i.e.* particle spectra, the parameter

$$k_0 = k, \tag{4}$$

in the model, is adjusted to a smaller value which could depend on excitation energy as well [36–43,48–50]. For our purposes we will use two fixed k_0 (we set $k_0 = k_{\text{infinity}}$ in GEMINI to achieve this) values of 7.3 MeV and 15 MeV since our goal is to test different methods to determine T and ρ from the model data. In fact, in the model, the temperature can be derived from eq. (2) if we stop the simulation after the first decay step. The following steps take into account a decreasing temperature due to particle emissions in previous decays, thus the T determination becomes "tricky" and we will discuss it later on in the paper. The model does not explicitly assume any density, even though one might simply think that the density of the system is that of the excited nucleus in its ground state density. This is not however correct since the Fermi-gas relation is assumed.

From eq. (4), $k_0 = 15$ MeV implies a nuclear ground-state density, while $k_0 = 7.3$ MeV results in $\frac{\rho}{\rho_0} = 0.34$. We stress here that other effects can be invoked to justify the smaller value of k_0, such as an effective mass or momentum dependence of the NEOS [36–43]; however in the simple Fermi-gas assumption used in the model, eq. (4) is the natural explanation. This has an important consequence and in fact, we would naively expect that the different approaches to determine the density will give values compatible to the estimate above, at least asymptotically (*i.e.* at high T where different effects, such as Coulomb barriers and Q-values become less important). At low T, these effects are important and will determine the probability of decay into a given channel rather than another. We anticipate that the decay probability at low T will effectively decrease the values of the densities obtained from all methods, which might correspond to the fact discussed in CoMD simulation, that the emitted particles at low T are located in a low density region of the nuclear surface: a low T will correspond to a lower ρ [22–26].

We also point out that the model assumes a barrier penetration of particles at various excitation energies [36–43]. An effective radius is assumed for the system: $R = (R_0 + 2.6)$ fm $= (1.16A^{1/3} + 2.6)$ fm. For a nucleus of mass $A = 80$, this gives an effective radius $R = 7.6$ fm which is equivalent to a system having a density less than one third of the normal nuclear density. Of course this assumption might be in contrast with the density value obtained from the Fermi-gas relation. However our goal is not to modify the model but to use it as a test bench, keeping in mind that these assumptions might be justified at low excitation energies (for which the model was proposed) and not at higher ones where fragmentation will dominate.

Before we apply DR, CF and QF methods to GEMINI data to extract temperature and density information, we briefly recall these methods here. For the DR method, the well known Saha equation gives the ratio of the density of two different fragments from the ratio of their yields [10]:

$$\frac{Y_1}{Y_2} = \left(\frac{A_1}{A_2}\right)^{\frac{3}{2}} \left(\frac{\lambda^3_{T,\mathcal{N}}}{2}\right)^{A_1 - A_2} \frac{2s_1 + 1}{2s_2 + 1} \times \rho_p^{Z_1 - Z_2} \rho_n^{N_1 - N_2} \exp\left[\frac{B_1 - B_2}{T}\right], \tag{5}$$

where $\lambda_{T,\mathcal{N}} = \frac{h}{\sqrt{2\pi m_0 T}}$ is the thermal wavelength, $\lambda^3_{T,\mathcal{N}} = 4.206 \times 10^3 (T/\text{MeV})^{-\frac{3}{2}}$ fm^3, s_i are the spins and B_i are the binding energies of the i-fragment. The ratio above depends on the unknown densities of proton (p) and neutron (n), as well as the temperature. We can write a similar

ratio for other fragments, for instance,

$$\frac{Y_3}{Y_4} = \left(\frac{A_3}{A_4}\right)^{\frac{3}{2}} \left(\frac{\lambda^3_{T,\mathcal{N}}}{2}\right)^{A_3-A_4} \frac{2s_3+1}{2s_4+1} \times \rho_p^{Z_3-Z_4} \rho_n^{N_3-N_4} \exp\left[\frac{B_3-B_4}{T}\right]. \quad (6)$$

Now, we have two equations but still three unknowns. A particular method to obtain the temperature was devised by Rubbino and collaborators [10], and consists in taking the ratio of eq. (5) and eq. (6):

$$\rho_p^{DZ}\rho_n^{DN} = \frac{\frac{Y_1Y_4}{Y_2Y_3}}{\left(\frac{A_1A_4}{A_2A_3}\right)^{\frac{3}{2}} \left(\frac{\lambda^3_{T,\mathcal{N}}}{2}\right)^{DA} \frac{(2s_1+1)(2s_4+1)}{(2s_2+1)(2s_3+1)} \exp\left[\frac{DB}{T}\right]}, \quad (7)$$

where $Df = (f_1+f_4)-(f_2+f_3)$. By imposing $DZ = (Z_1+Z_4)-(Z_2+Z_3) = 0$ and $DN = (N_1+N_4)-(N_2+N_3) = 0$ we can eliminate the densities from eq. (7). The equation can be inverted to obtain T, since the binding energies of the fragments are well known. Once the T is obtained, we can substitute it into eqs. (5) and (6) to calculate the density if we choose the right combination of fragments. In our case, we choose two combinations: d, t, ^{3}He, α (dthα) and p, n, t, ^{3}He (pnth).

In [21] it was proposed to look at quadrupole fluctuations in momentum space to determine the classical temperature. The quadrupole momentum (Q_{xy}) in the transverse direction was defined in order to minimize non-equilibrium effects:

$$Q_{xy} = p_x^2 - p_y^2, \quad (8)$$

where p_x and p_y are the transverse components of a given fragment's momentum. In the classical case, *i.e.* Maxwell distribution, the temperature and density are decoupled, thus the quadrupole momentum fluctuation properly normalized is only a function of T:

$$\langle Q_{xy}^2\rangle = (2mT)^2. \quad (9)$$

Since $\langle Q_{xy}^2\rangle$ can be calculated from data, we can derive the temperature T from eq. (9). If we use the Fermi-Dirac distribution for fermions to calculate the quadrupole momentum fluctuations, our results will depend on the chemical potential μ as well. We need another condition which we choose to be the multiplicity fluctuations. This choice is dictated by the fact that multiplicity fluctuations are equal to one for a classical ideal system, while for fermions (bosons) are smaller (larger, near and above the critical point for BEC) than one [31–34]. For fermions we get [23]

$$\langle Q_{xy}^2\rangle = (2mT)^2\left[0.2\left(\frac{T}{\varepsilon_f}\right)^{-1.71}+1\right], \quad (10)$$

$$\frac{T}{\varepsilon_f} = -0.442 + \frac{0.442}{\left(1-\frac{\langle(\Delta N)^2\rangle}{\bar{N}}\right)^{0.656}} + 0.345\frac{\langle(\Delta N)^2\rangle}{\bar{N}} - 0.12\left(\frac{\langle(\Delta N)^2\rangle}{\bar{N}}\right)^2. \quad (11)$$

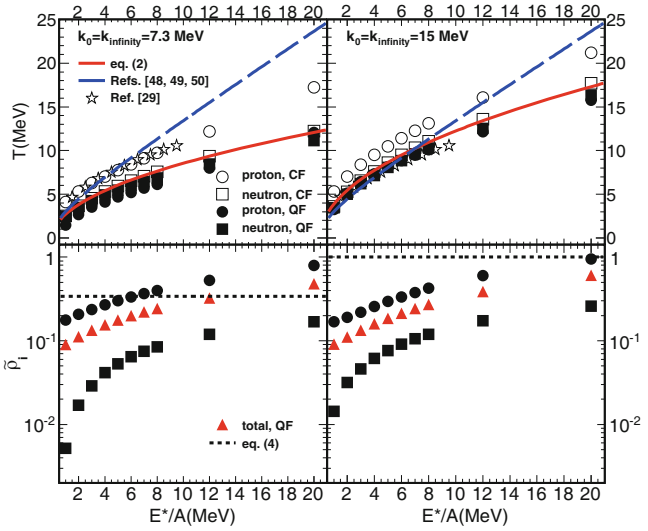

Fig. 1. (Color online) Temperature (top panels) and scaled density (bottom panels) as function of the excitation energy per particle. Different values of k_0 are used in the left and right panels.

Since we can measure the normalized multiplicity fluctuations $\frac{\langle(\Delta N)^2\rangle}{\bar{N}}$, then we can obtain $\frac{T}{\varepsilon_f}$ from eq. (11). Substituting $\frac{T}{\varepsilon_f}$ into eq. (10), we obtain the temperature T, then the Fermi energy ε_f. The density can be determined with the Fermi energy relation $\varepsilon_f = 36(\frac{4}{g}\frac{\rho}{\rho_0})^{2/3}$ MeV where g is the degeneracy of the particle and $\rho_0 = 0.16\,\mathrm{fm}^{-3}$.

3 Results and discussions

Using the GEMINI code available in the literature [36–43], we have generated one million events for each excitation energy (or initial T). First we discuss the results for the simulations stopped at the first decay step where the relation of the excitation energy and temperature is given by eq. (2). In fig. 1 we plot the temperature T (top panels) and the scaled density $\tilde{\rho}_{i0} = \frac{\rho_i}{\rho_{i0}}$, where $i = p, n, p+n$ and $\rho_{p0} = \rho_{n0} = 0.08\,\mathrm{fm}^{-3}$, $\rho_0 = 0.16\,\mathrm{fm}^{-3}$, (bottom panels) as function of the excitation energy per particle of the initial hot system. Two different values of the k_0 Fermi-gas parameter are used in the left and right panels. The "exact" value of T obtained from the Fermi-gas relation, eq. (2), is given by the full (red) lines. Available experimental data from the current literature are given by the dashed (blue) lines [48–50] and open stars [29], which we have reported for reference purposes only. The quantum fluctuation (QF) method, both for neutron and proton, agrees rather well with the exact result as expected since the basic assumption in the method and in the GEMINI model is the same, *i.e.* a nucleus made of fermions. The classical fluctuation (CF) method agrees with the exact method especially for the neutron case and at low excitation energies for both protons and neutrons [44, 45]. The reason for this behavior could be explained from the

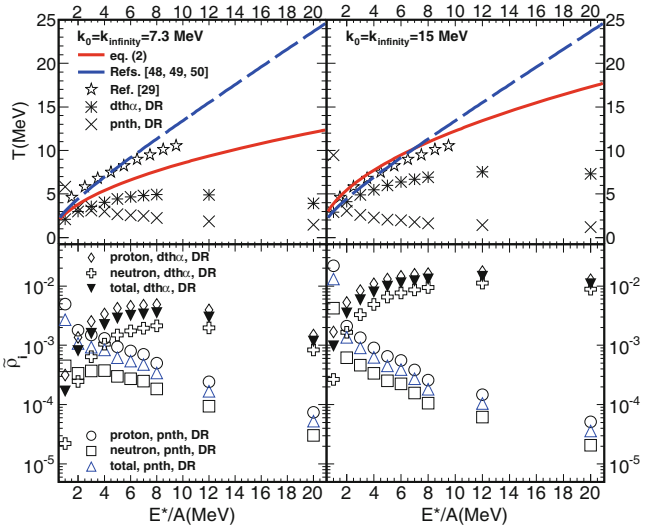

Fig. 2. (Color online) Same as in fig. 1. The results are for dthα DR and pnth DR.

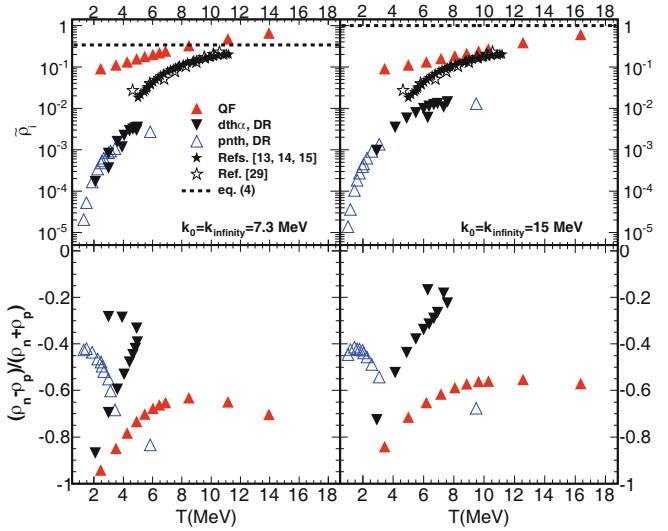

Fig. 3. (Color online) The total scaled densities (top panels) and density differences between neutrons and protons (bottom panels) as a function of the temperature.

bottom part of fig. 1. The densities estimated only from the QF method (the CF does not determine a density since the multiplicity fluctuation are equal to one classically) are very low especially for neutrons. We expect that at low densities and relatively high T, classical and quantum methods should give similar results. As we will show the density obtained using the DR method is even smaller than the one obtained from QF. In fig. 1, the proton scaled density is given by full circles and the neutron scaled density by full squares, while the total scaled density is given by full triangle symbols. The reason for which we have extended the model to such high excitation energies where it is not necessarily justified, is because we wanted to show that the estimated total density tends asymptotically to the value estimated from the Fermi-gas relation, eq. (4), using the respective k_0 values which are given by the dotted horizontal lines in fig. 1. At low excitation energies, different Q-values for particle emissions and barrier penetrations modify the fluctuations given by the Fermi-gas entropy, eq. (1), which results in lower densities as displayed. If these effects would be turned off, then fluctuations would arise from the Fermi-gas entropy as for the QF method which is based on the same Fermi-gas assumption [46].

The discussion above can be extended to the DR method [6–15] and is reported in fig. 2. Two DR particle combinations (dthα and pnth) are shown in the figure. The celebrated plateau of the caloric curve is observed in fig. 2 (top panels) especially for the dthα combination mostly used in the literature [7, 51]. Notice the peculiar and maybe surprising result obtained using the pnth DR for which T goes down for increasing excitation energy (top panels in fig. 2). A similar opposite behavior for the two cases is obtained for the densities (bottom panels in fig. 2). In particular the pnth densities decrease for increasing excitation energy. All densities estimated from DR are much smaller than those from QF (see fig. 1) and do not asymptotically tend to the value obtained from the Fermi-gas relation, eq. (4). Of course this is not surprising since we are using classical physics to estimate quantities obtained from a model based on a quantum (Fermi-gas) system.

Another way to visualize the results is by plotting scaled density (top panels) and the difference of neutron and proton density (bottom panels) as function of T as reported in fig. 3. Now the surprising differences in the densities obtained from the dthα and pnth cases in fig. 2 are not observed: the two DR methods agree which simply tells us that the control parameter is T and not the excitation energy as it should be in a statistical model. The densities differ greatly in the QF and DR methods as observed before. Equation (4) and the available data support higher densities [13–15, 20, 29]. In ref. [20] a similar discussion is reported and it was concluded that QF and coalescence methods are better justified because quantum effects become more important with increasing densities as expected. Furthermore the QF results tend asymptotically to the value expected from the Fermi-gas and the used k_0 parameters. Notice the large difference between n and p densities as obtained in different approaches (bottom panels in fig. 3). In particular all different methods fail to reproduce the initial source value of zero ($N = Z$) which should be recovered at high T. This is however a failure of the statistical model which we have pushed at high excitation energies where it is not justified. We recall that in a two-component system phase transition, the quantity plotted in the bottom part of fig. 3, could be considered as an order parameter [52, 53].

For completeness, in figs. 4 and 5, we display the results obtained when all steps in the statistical decay model are taken into account. These figures should be compared to figs. 1 and 2, respectively. We observe generally a decrease of T and an increase of ρ compared to the first step results. This result implies that, if the general assumption of a sequential decay is correct, then the derived T and

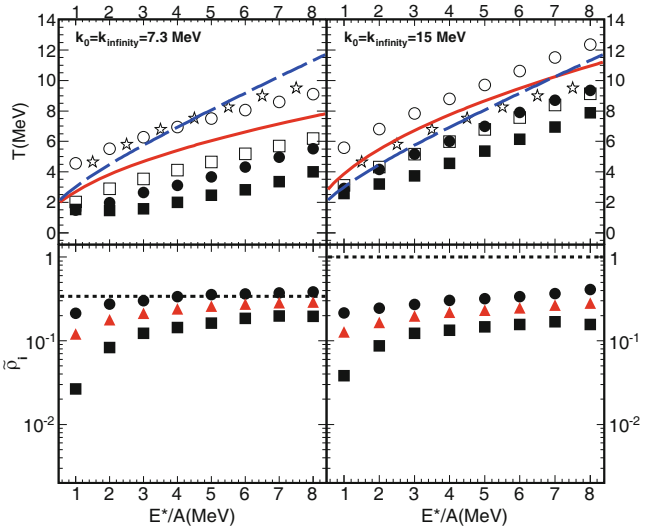

Fig. 4. (Color online) Same as fig. 1 for all steps model simulations.

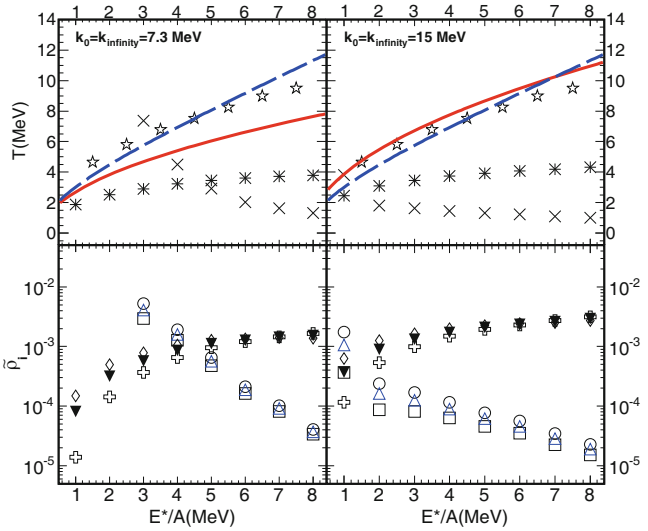

Fig. 5. (Color online) Same as fig. 2 for all steps model simulations.

ρ estimated in the different methods are effective values influenced by the secondary decay. Within the fluctuation method, it seems that the initial T is somehow between the classical and the quantum cases, while the DR method fail in all cases. However, as we have seen in fig. 3, plots of ρ and T as function of excitation energy might be misleading as in the dthα and pnth cases. In fig. 6 we plot ρ as function of T obtained from different assumptions both at the first decay and all decay steps. As we see in the figure, the results from the DR method roughly collapse in a single curve, which suggests that indeed the values of T might shift down due to the secondary decay, however the corresponding density is also modified in such a way to collapse in a single curve. This result should be compared to similar calculations using CoMD, see fig. 26 in ref. [2].

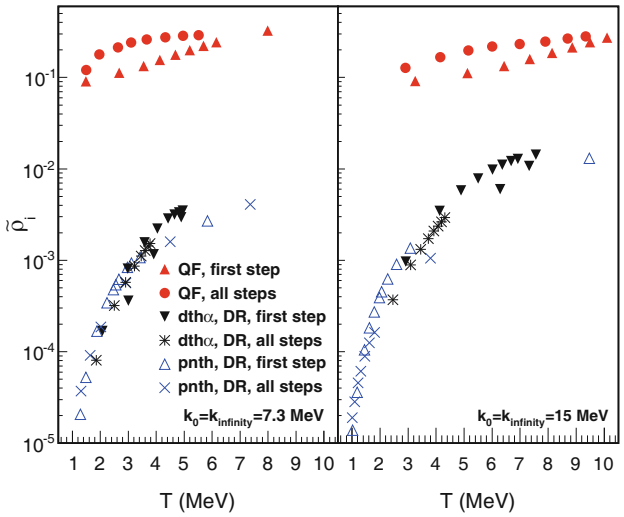

Fig. 6. (Color online) Total scaled density for first step and all steps model simulations *vs.* temperature.

4 Conclusions

In conclusion, in this paper we have compared different proposed methods to extract density and temperature using a statistical sequential model. We have shown that the model observables are better reproduced by the quantum fluctuations method since the same physical ingredient, the Fermi gas, is used. Double ratios fail because of the classical assumptions as it should be. However, the feature that different ratios give different T and ρ as function of excitation energy is misleading. Notice that if different particles are emitted at different times and/or from different sources, then one could obtain different densities and/or temperatures. An agreement of the different particle ratios is observed when the temperature is used as a control parameter as it should be in a statistical environment. Secondary decays support again the QF method as compared to the DR and differences might be highlighted by plotting densities as function of the control parameter T.

We thank prof. J. Natowitz for stimulating discussions.

References

1. B.A. Li, L.W. Chen, C.M. Ko, Phys. Rep. **464**, 113 (2008).
2. G. Giuliani, H. Zheng, A. Bonasera, Progr. Part. Nucl. Phys. **76**, 116 (2014).
3. V. Baran, M. Colonna, V. Greco, M. Di Toro, Phys. Rep. **410**, 335 (2005).
4. A.W. Steiner, M. Prakash, J.M. Lattimer, P.J. Ellis, Phys. Rep. **411**, 325 (2005).
5. J.M. Lattimer, M. Prakash, Phys. Rep. **442**, 109 (2007).
6. A. Bonasera, M. Bruno, C.O. Dorso, P.F. Mastinu, Riv. Nuovo Cimento **23**, 2 (2000).
7. J.B. Natowitz *et al.*, Phys. Rev. C **65**, 034618 (2002).
8. A. Kelić, J.B. Natowitz, K.H. Schmidt, Eur. Phys. J. A **30**, 203 (2006).

9. M.B. Tsang, F. Zhu, W.G. Lynch, A. Aranda, D.R. Bowman, R.T. de Souza, C.K. Gelbke, Y.D. Kim, L. Phair, S. Pratt, C. Williams, H.M. Xu, W.A. Friedman, Phys. Rev. C **53**, R1057 (1996).
10. S. Albergo, S. Costa, E. Costanzo, A. Rubbino, Nuovo Cimento A **89**, 1 (1985).
11. S. Das Gupta, J. Pan, M.B. Tsang, Phys. Rev. C **54**, R2820 (1996).
12. H. Xi, W.G. Lynch, M.B. Tsang, W.A. Friedman, D. Durand, Phys. Rev. C **59**, 1567 (1999).
13. L. Qin *et al.*, Phys. Rev. Lett. **108**, 172701 (2012).
14. K. Hagel *et al.*, Phys. Rev. Lett. **108**, 062702 (2012).
15. R. Wada *et al.*, Phys. Rev. C **85**, 064618 (2012).
16. A. Mekjian, Phys. Rev. Lett. **38**, 640 (1977).
17. A.Z. Mekjian, Phys. Rev. C **17**, 1051 (1978).
18. T.C. Awes, G. Poggi, C.K. Gelbke, B.B. Back, B.G. Glagola, H. Breuer, V.E. Viola, Jr., Phys. Rev. C **24**, 89 (1981).
19. L.P. Csernai, J.I. Kapusta, Phys. Rep. **131**, 223 (1986).
20. G. Röpke, S. Shlomo, A. Bonasera, J.B. Natowitz, S.J. Yennello, A.B. McIntosh, J. Mabiala, L. Qin, S. Kowalski, K. Hagel, M. Barbui, K. Schmidt, G. Giulani, H. Zheng, S. Wuenschel, Phys. Rev. C **88**, 024609 (2013).
21. S. Wuenschel *et al.*, Nucl. Phys. A **843**, 1 (2010).
22. H. Zheng, A. Bonasera, Phys. Lett. B **696**, 178 (2011).
23. H. Zheng, A. Bonasera, Phys. Rev. C **86**, 027602 (2012).
24. H. Zheng, G. Giuliani, A. Bonasera, Nucl. Phys. A **892**, 43 (2012).
25. H. Zheng, G. Giuliani, A. Bonasera, Phys. Rev. C **88**, 024607 (2013).
26. H. Zheng, G. Giuliani, A. Bonasera, J. Phys. G: Nucl. Part. Phys. **41**, 055109 (2014).
27. M. Papa, T. Maruyama, A. Bonasera, Phys. Rev. C **64**, 024612 (2001).
28. M. Papa, G. Giuliani, A. Bonasera, J. Comput. Phys. **208**, 403 (2005).
29. J. Mabiala, A. Bonasera, H. Zheng, A.B. McIntosh, Z. Kohley, P. Cammarata, K. Hagel, L. Heilborn, L.W. May, A. Raphelt, G.A. Souliotis, A. Zarrella, S.J. Yennello, Int. J. Mod. Phys. E **22**, 1350090 (2013).
30. B.C. Stein *et al.*, J. Phys. G: Nucl. Part. Phys. **41**, 025108 (2014).
31. J. Esteve *et al.*, Phys. Rev. Lett. **96**, 130403 (2006).
32. T. Müller *et al.*, Phys. Rev. Lett. **105**, 040401 (2010).
33. C. Sanner *et al.*, Phys. Rev. Lett. **105**, 040402 (2010).
34. C.I. Westbrook, Physics **3**, 59 (2010).
35. P. Marini *et al.*, in preparation.
36. R.J. Charity, Computer code GEMINI, see `http://www.chemistry.wustl.edu/~rc`.
37. J.O. Newton, D.J. Hinde, R.J. Charity, J.R. Leigh, J.J.M. Bokhorst, A. Chatterjee, G.S. Foote, S. Ogaza, Nucl. Phys. A **483**, 126 (1988).
38. R.J. Charity *et al.*, Nucl. Phys. A **483**, 371 (1988).
39. D.R. Bowman, G.F. Peaslee, N. Colonna, R.J. Charity, M.A. McMahan, D. Delis, H. Han, K. Jing, G.J. Wozniak, L.G. Moretto, W.L. Kehoe, B. Libby, A.C. Mignerey, A. Moroni, S. Angius, I. Iori, A. Pantaleo, G. Guarino, Nucl. Phys. A **523**, 386 (1991).
40. R.J. Charity, Phys. Rev. C **53**, 512 (1996).
41. R.J. Charity, Phys. Rev. C **61**, 054614 (2000).
42. L.G. Sobotka, R.J. Charity, J.Tõke, W.U. Schröder, Phys. Rev. Lett. **93**, 132702 (2004).
43. R.J. Charity, Phys. Rev. C **82**, 014610 (2010).
44. W.D. Tian, Y.G. Ma, X.Z. Cai, D.Q. Fang, W. Guo, W.Q. Shen, K. Wang, H.W. Wang, M. Veselsky, Phys. Rev. C **76**, 024607 (2007).
45. P. Zhou, W.D. Tian, Y.G. Ma, X.Z. Cai, D.Q. Fang, H.W. Wang, Phys. Rev. C **84**, 037605 (2011).
46. L. Landau, F. Lifshits, *Statistical Physics* (Pergamon, New York, 1980).
47. K. Huang, *Statistical Mechanics*, second edition (J. Wiley and Sons, New York, 1987).
48. L.G. Moretto, J.B. Elliott, L. Phair, P.T. Lake, J. Phys. G: Nucl. Part. Phys. **38**, 113101 (2011).
49. J.B. Elliott, P.T. Lake, L.G. Moretto, L. Phair, Phys. Rev. C **87**, 054622 (2013).
50. J.B. Elliott *et al.*, Phys. Rev. C **67**, 024609 (2003).
51. J. Pochodzalla *et al.*, Phys. Rev. Lett. **75**, 1040 (1995).
52. A. Bonasera *et al.*, Phys. Rev. Lett. **101**, 122702 (2008).
53. J. Mabiala *et al.*, in preparation.